BRAIN
ORIGINAL ARTICLE

A direct spinal cord–computer interface enables the control of the paralysed hand in spinal cord injury

Daniela Souza Oliveira,[1,†] Matthias Ponfick,[2] Dominik I. Braun,[1] Marius Osswald,[1] Marek Sierotowicz,[1,3] Satyaki Chatterjee,[1] Douglas Weber,[4,5] Bjoern Eskofier,[1,6] Claudio Castellini,[1,3] Dario Farina,[7] Thomas Mehari Kinfe[1,8,‡] and Alessandro Del Vecchio[1,†,‡]

[†,‡]These authors contributed equally to this work.

Paralysis of the muscles controlling the hand dramatically limits the quality of life for individuals living with spinal cord injury (SCI). Here, with a non-invasive neural interface, we demonstrate that eight motor complete SCI individuals (C5–C6) are still able to task-modulate in real-time the activity of populations of spinal motor neurons with residual neural pathways.

In all SCI participants tested, we identified groups of motor units under voluntary control that encoded various hand movements. The motor unit discharges were mapped into more than 10 degrees of freedom, ranging from grasping to individual hand-digit flexion and extension. We then mapped the neural dynamics into a real-time controlled virtual hand. The SCI participants were able to match the cue hand posture by proportionally controlling four degrees of freedom (opening and closing the hand and index flexion/extension).

These results demonstrate that wearable muscle sensors provide access to spared motor neurons that are fully under voluntary control in complete cervical SCI individuals. This non-invasive neural interface allows the investigation of motor neuron changes after the injury and has the potential to promote movement restoration when integrated with assistive devices.

1 Department Artificial Intelligence in Biomedical Engineering, Friedrich-Alexander-Universität Erlangen-Nürnberg, 91052 Erlangen, Germany
2 Querschnittzentrum Rummelsberg, Krankenhaus Rummelsberg GmbH, 90592 Schwarzenbruck, Germany
3 Institute of Robotics and Mechatronics, German Aerospace Center (DLR), 82234 Oberpfaffenhofen, Germany
4 Department of Mechanical Engineering, Carnegie Mellon University, Pittsburgh, PA 15213, USA
5 Neuroscience Institute, Carnegie Mellon University, Pittsburgh, PA 15213, USA
6 Translational Digital Health Group, Institute of AI for Health, Helmholtz Zentrum München—German Research Center for Environmental Health, 85764 Neuherberg, Germany
7 Department of Bioengineering, Imperial College London, London, SW7 2AZ, UK
8 Division of Functional Neurosurgery and Stereotaxy, Friedrich-Alexander-Universität Erlangen-Nürnberg, 91054 Erlangen, Germany

Received December 24, 2022. Revised January 24, 2024. Accepted March 05, 2024. Advance access publication March 19, 2024

Correspondence to: Alessandro Del Vecchio
Department Artificial Intelligence in Biomedical Engineering
Faculty of Engineering, Friedrich-Alexander-Universität Erlangen-Nürnberg
Henkestraße 91, 91052 Erlangen, Germany
E-mail: alessandro.del.vecchio@fau.de

Correspondence may also be addressed to:
Daniela Souza de Oliveira
E-mail: daniela.s.oliveira@fau.de

Keywords: spinal cord injury; motor neuron; motor unit; high density surface electromyography; neural interface

Introduction

Impaired hand function is arguably one of the most severe motor deficits in subjects with spinal cord injury (SCI), especially when bilateral.[1] There are currently no effective treatments for regaining hand control after muscle paralysis. Hand surgery is established, although not possible in every case, and with several challenges, such as reconstruction of intrinsic hand function and requiring precise diagnostics and planning.[2] Restoration of hand function has so far been achieved by neural interfaces recording the activity of the motor cortex,[3] either through closed-loop electrical stimulation of the muscle[4] or by controlling external devices.[5] However, besides the relatively poor control, invasive cortical implants are also an option limited to a small proportion of patients because of the surgical risks and long-term stability of the implant. Other neural interfaces involve the delivery of electrical stimulations in the spinal cord that indirectly target the activity of the alpha motor neurons.[6]

The neural information most directly associated with behaviour is the activity of spinal alpha motor neurons, representing the final neural code of movement. The activity of spinal motor neurons generates movement through a simple transformation (the dynamics of the twitch forces of the muscle units), and therefore, movement intent can be decoded directly. Almost all SCIs are due to contusions of the spinal cord, which could leave some spared connections above and below the level of the injury.[7] While this spared neural activity is insufficient to drive muscles to generate detectable forces, it can be used to infer motor intent and, therefore, to decode movements. Accordingly, as a case study, we have recently reported in a single motor-complete SCI (C5–C6) individual the presence of a significant number of task-modulated motor units encoding the flexion and extension of individual fingers through a wearable, non-invasive neural interface.[8] That case study was a proof of concept in a single patient, and it was limited to offline analysis without any demonstration of patient-in-the-loop control. Here, we support previous evidence of voluntarily controlled spinal motor neurons in eight SCI individuals (injury levels ranging from C5 to C6).[7-10] Through the decomposition of the high-density surface electromyogram (HDsEMG),[11-13] we identified active motor neurons in all tested patients (Fig. 1). These motor neurons encoded the movements of the paralysed hand during synergistic and individual digit movements. The discharge patterns of the motor neurons were similar to those observed in non-injured young adults. The motor neurons followed precise recruitment and discharge rate patterns that closely matched the movements of the virtual hand. This study shows that even many years after chronic SCI, there are still spared motor neurons that receive functional inputs modulated by voluntary intent.

Materials and methods

Participants

Eight participants with SCI were recruited for this study (seven individuals with chronic motor complete SCI and one with motor incomplete SCI—Fig. 2 and Table 1). The inclusion criteria were: (i) injury level C4–C6; (ii) aged between 18 and 60 years old; and (iii) absence of voluntary movement of one hand or both hands. Two participants (Subjects S6 and S7) had functional left hands.

In Table 1, we report information from standard clinical examinations of the SCI group regarding clinical classification of injury according to the American Spinal Injury Association (ASIA) impairment scale; spasticity assessment through the modified Ashworth scale and testing of upper limb stretch reflexes (biceps, triceps and brachioradialis tendon reflexes). In Supplementary Fig. 1, we provide T2-weighted MRI images from the SCI group's medical history to depict the location and diversity of the injuries.

Additionally, we recruited 12 healthy, uninjured subjects (control group, age 27.1 ± 3.4 years, two females) for comparison.

All participants gave their written informed consent to take part in the study. The study was conducted in agreement with the Declaration of Helsinki and was approved by the Friedrich-Alexander-Universität Ethics Committee (applications 22-138-Bm and 21-150-B).

Study overview and experimental protocol

This study was conducted in two sessions. In the first session, we asked the participants to attempt the movements displayed by videos of a virtual hand. At the same time, we recorded HDsEMG signals from their forearm muscles. For the second session, six participants from the SCI group returned after 3–5 months of the first session (Subjects S1–S4, S6 and S8), in which a regression model (based on global EMG) and/or an online decomposition method was used to decode movement intention, according to their HDsEMG signals.

In the first session, according to their forearm circumference, we placed 256 or 320 HDsEMG electrodes on the forearm of the participants' dominant hand (Subject S7 was paralysed only on the non-dominant hand). The electrodes covered the forearm muscles and the wrist. We chose this placement to maximize the number of electrodes and, thus, improve the accuracy of HDsEMG decomposition since we can also detect far-field electrical potentials at the wrist.[14] For the SCI group, after placing the electrodes, we asked the subjects to stay in a comfortable position with their arms (Figs 1A and and see later). For the control group, the participants were standing with their dominant elbows flexed (this setup was previously described[15]). To both groups, we showed the same video

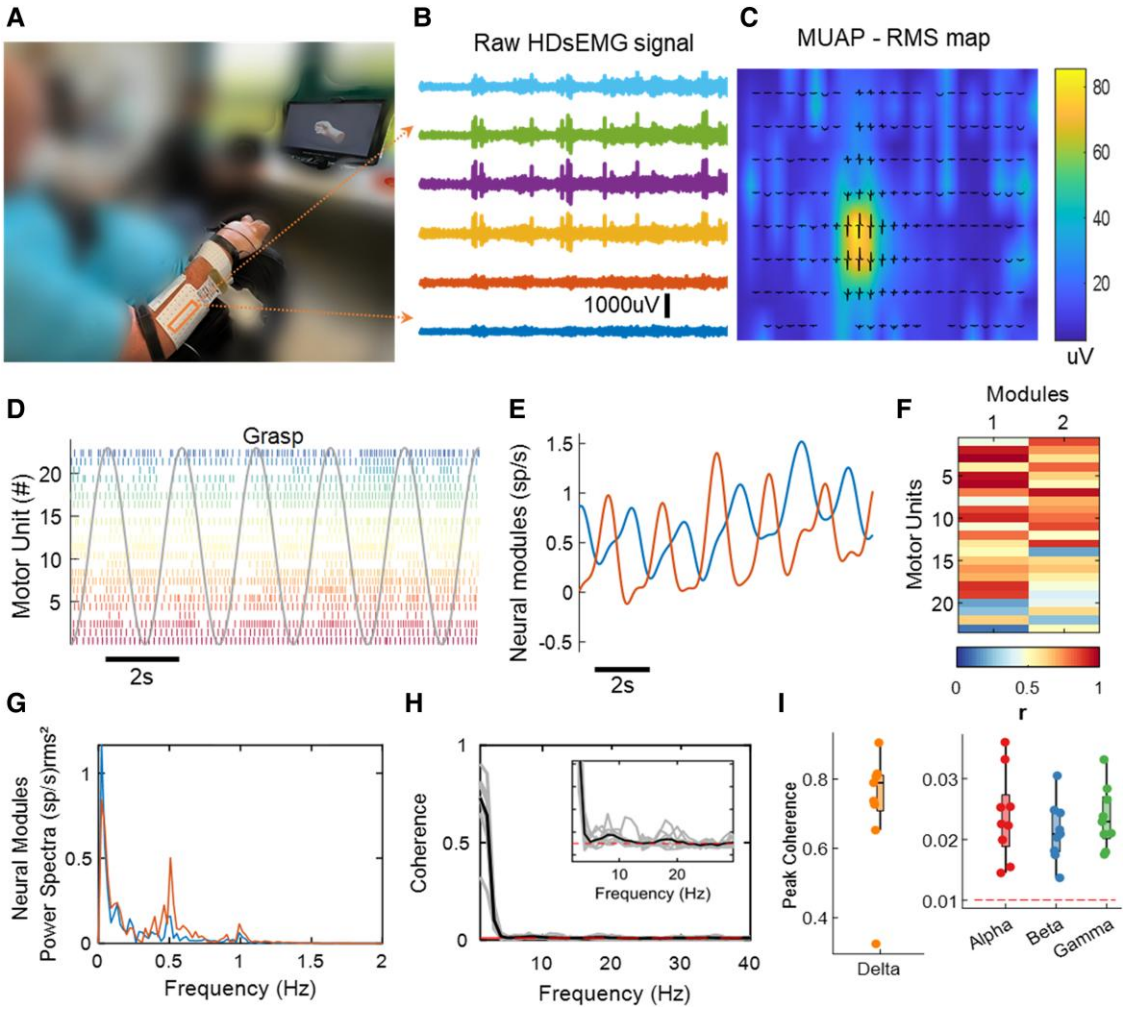

Figure 1 Overview of experimental setup and motor unit data analysis. (**A**) Experimental setup consisting of 320 surface electromyogram (EMG) electrodes placed in the forearm muscles. The movement instructions were guided by a virtual hand video displayed on a monitor in front of the subject. (**B**) A few example electrodes show raw high-density surface EMG (HDsEMG) signals while the subject attempts a grasp task (flexion and extension of the fingers, 0.5 Hz). (**C**) Example of spatial mapping based on the root mean square (RMS) values of the motor unit action potential (MUAP). (**D**) Raster plot of motor unit firings (colour-coded) identified during 10 s of a grasp task. (**E**) Neural modules extracted for the same task, using factorization analysis. (**F**) Pearson correlation values (*r*) of the individual motor units with the two neural modules. (**G**) Neural modules' power spectra, showing a peak at the movement frequency (0.5 Hz). (**H**) Coherence between cumulative spike trains of motor units across all tasks of Subject 6 (S6), highlighting alpha and beta bands. (**I**) Coherence peak across all tasks of Subject S6 for delta (1–5 Hz), alpha (6–12 Hz), beta (15–30 Hz) and gamma (31–80 Hz) bandwidths. The dashed line in red in **H** and **I** indicates the coherence threshold (average coherence between 100–250 Hz).

of a virtual hand performing different tasks on a computer monitor and instructed the participants to attempt the movements accordingly. The tasks lasted 42 s each and included flexion and extension of the individual digits at two speeds (0.5 and 1.5 Hz), grasp, two-finger pinch, three finger pinch, and wrist flexion and extension (0.5 Hz). Two trials were performed for each movement (only for the SCI group). We only analysed data from slow (0.5 Hz) movements as the subjects reported difficulty performing the fast ones.

In the second session, we tested a real-time EMG decomposition approach (brief offline decomposition followed by online decomposition, see later). We used 128 HDsEMG electrodes to assess if the subjects would be able to follow a digital trajectory with their motor units smoothed cumulative discharge rate. First, during the offline decomposition, we recorded HDsEMG data while the participants attempted a maximum flexion of the digits (10 s per task). These data were decomposed as described in the 'Online decomposition' section in the Supplementary material, and we stored the decomposition results for the online task.

Subsequently, in the online decomposition step, we instructed the subjects to follow a periodic rectangular waveform trajectory shown on a monitor, with 10 s periods (5 s of rest in between), for 60–120 s. The trajectories had two different activation levels, 20% and 30% of maximum neural activation, i.e. of the maximum discharge rate obtained during the brief offline decomposition step. These activation values should not be confused with the maximal voluntary force obtained in healthy individuals. It could be impossible for a person to modulate the discharge rate of a specific motor unit up to its maximum for a prolonged time. This is because of the non-linear behaviour of motor units due to the spike frequency adaptation and the discharge rate modulation due to intrinsic motor neuron properties.[16-18]

The subjects attempted flexion and extension of the same digits for two consecutive periods as performed in the offline decomposition with 20% maximum neural activation. The motor unit firings detected with this method (smoothed motor unit firings) were shown as feedback to the subjects. Lastly, we tested whether the

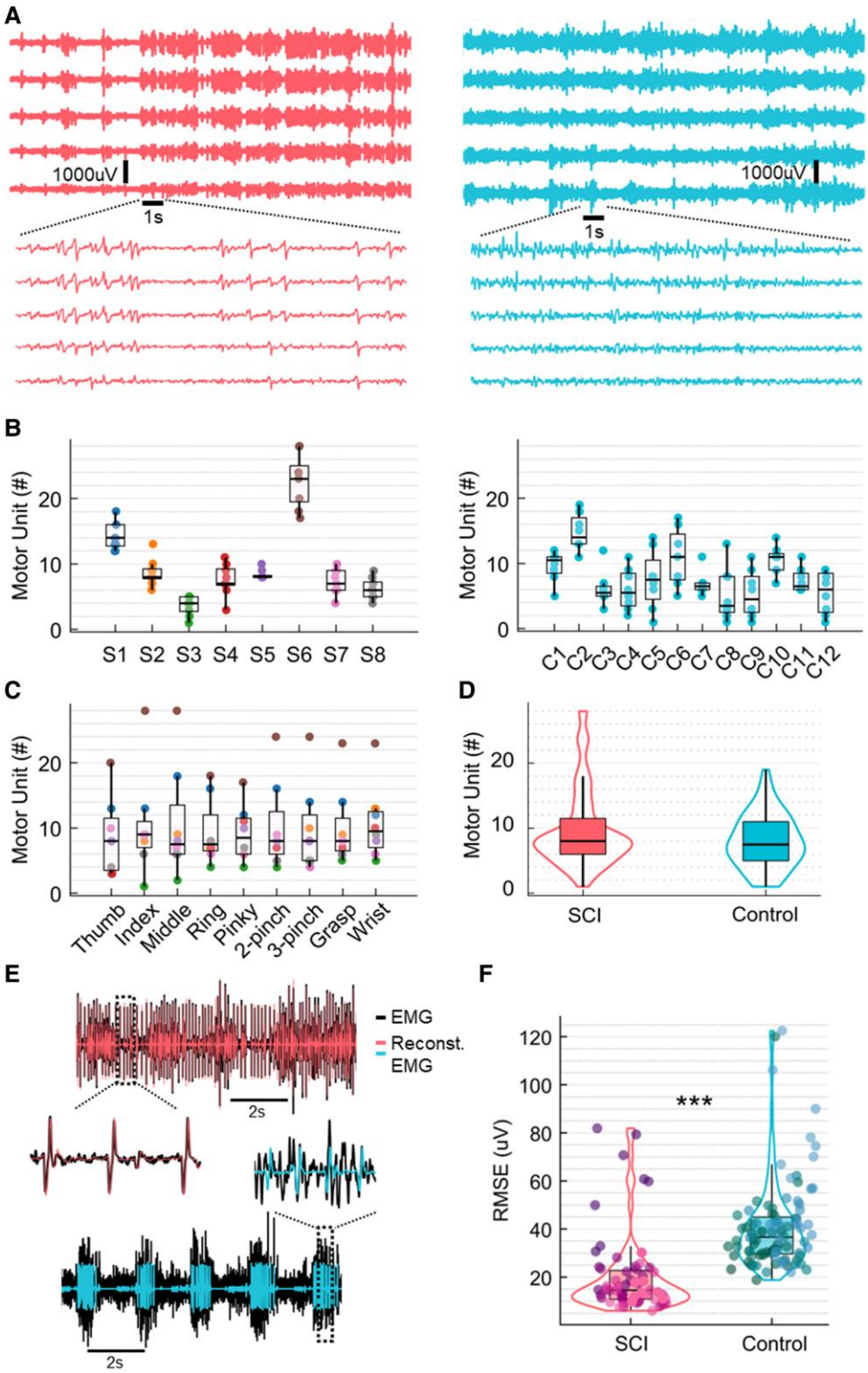

Figure 2 Number of detected motor units and residual high-density surface electromyogram signals. (**A**) Example of raw high-density surface electromyogram (HDsEMG) signals for both groups, spinal cord injury (SCI; *left*) and control (*right*). The signals are shown in time windows of 20 and 1 s. (**B**) Number of detected motor units across subjects for both groups, SCI and control (the dots are colour-coded for the subjects of the SCI group). (**C**) Number of detected motor units across all tasks (the dots represent the tasks). (**D**) Distribution of the total number of motor units across groups, SCI (*left*) and control (*right*). (**E**) Example of EMG channels from both SCI and control groups overlayed with the reconstructed EMG. (**F**) Root mean square error (RMSE) between EMG and reconstructed EMG, representing the residual EMG activity for both groups. ***$P < 0.001$.

Table 1 Characteristics of research participants

Subject	Age, years	Gender	Injury level	AIS	Wrist movement	Time since injury, years	Sensory level[a]	Spasticity upper limb, MAS[b]	Note	Stretch reflexes upper limb	MUs/task[c]	Unique MUs/task[c]
S1	39	Male	C6	B	Yes	18.8	S5	0	Tenodesis	Absent	14.5 ± 2	10.1 ± 2.3
S2	34	Male	C5	B	Yes	9.1	C5	0	Tenodesis	B: reduced; BR, T: absent	8.1 ± 1.2	5.7 ± 1.7
S3	41	Female	C6	B	Yes	24.2	C6	0	Tenodesis	B, BR: exaggerated; T: absent	3.5 ± 1.4	0.8 ± 1.6
S4	39	Female	C5	A	Yes	24.2	C5	0	–	Normal	7.3 ± 2.3	3.7 ± 1.3
S5	34	Male	C6	A	No	22.2	C6	0	–	Absent	8.4 ± 0.7	8.3 ± 0.7
S6	57	Male	C5	A	No	6.9	T3	Right: 2, left: 0	Botox right arm	Right: reduced; left: exaggerated	22.8 ± 4.2	21.1 ± 3.2
S7	44	Male	C6	C	No	18.2	C6	Right: 2, left: 0	–	Right: exaggerated; left: reduced	7.4 ± 2	4.4 ± 2.7
S8	38	Female	C5	B	Yes	5.0	T1	1	–	Absent	5.9 ± 1.2	4.8 ± 1.6

AIS = ASIA Impairment Scale; B = biceps reflex; BR = brachioradialis reflex; MAS = Modified Ashworth Scale; T = triceps reflex.
[a]The sensory level corresponds to lowest level with normal sensory function.
[b]Spasticity was assessed for elbow flexion.
[c]Average number of motor units (MUs) identified per task (mean ± standard deviation) for each subject.

participants could modulate their discharge rate and progressively recruit motor units by increasing the height of the ramp to 30% maximum neural activation and alternating between the two activation levels (Supplementary Video 1).

Also, an EMG-to-activation regression model was generated in the second session using the same electrode configuration as in the first visit. During this session, we asked the subjects to indicate which tasks from the first session they could perform with the least effort. These tasks were, therefore, selected to build the model. For that, the subjects were asked to attempt the maximal/full flexion of these tasks (e.g. the selected task was index movement; thus, they had to perform an index maximal flexion to build the model). These EMG signals were acquired and associated to the synthetic ground truth representing maximal activation for the relevant degrees of freedom (df). After that, the participants attempted the flexion and extension of the digits according to their chosen tasks. The predicted activation was shown in real-time through a virtual hand interface ('predicted hand'; see later and Supplementary Video 2). We used a virtual hand showing a predefined movement (referred to here as 'control hand'; see later) to help the subjects to perform the movements and for further analysis.

For complete information about the recordings and data analysis, see the Supplementary material.

Results

To assess the extent of spared motor unit activity in SCI participants, we analysed the number of identified motor units, the reconstructed HDsEMG signals (motor unit action potential shapes convolved with motor unit firings), discharge rate and coherence area values. We compared these measures to those of the control group. Additionally, we evaluated the outcomes of the real-time decomposition and virtual hand control.

Figure 1 shows an overview of the offline experiments. We asked the subjects to match the visual cue displayed through a virtual hand (hand opening and closing, two and three finger pinch and flexion and extension of individual digits at 0.5 Hz movement velocity). Figure 1A shows the experimental setup, with 320 electrodes placed on the proximal and distal forearm muscles and tendons (wrist). Figure 1B and C illustrates six EMG channels and a motor unit waveform superimposed on a heat map based on the root mean square activity. In all tested patients, we observed clear motor unit action potentials with high signal-to-noise ratio (>26 dB[19]). We then looked at how these motor units were controlled by studying the association between motor unit activation times (Fig. 1D) and the attempted movement by looking at the trajectories of the digit tip of the virtual hand (grey curve in Fig. 1D). The raster plot in Fig. 1D shows a clear grouping of motor units encoding flexion and extension movements during a grasping task. As in our previous experiment,[8] we used a factorization method to retrieve the motor dimension (flexion and extension of the motor units; Figs 1E and F). For all tested individuals, we consistently identified some motor neurons that were controlling the flexion and extension movements (Supplementary Figs 2–9). From the power spectrum of the neural modules (Fig. 1G), we found a peak at the movement frequency 0.5 Hz and lower frequencies. Figure 1H and I shows the coherence values across all tasks of Subject S6 (mean) and the coherence peak for the delta (1–5 Hz), alpha (6–12 Hz), beta (15–30 Hz) and gamma (31 –80 Hz) bandwidths.

Table 1 and Supplementary Fig. 1 show a summary of all subjects and tasks, including a description of the SCI through T2-weighted MRI. Details regarding the sensory level of the injury,

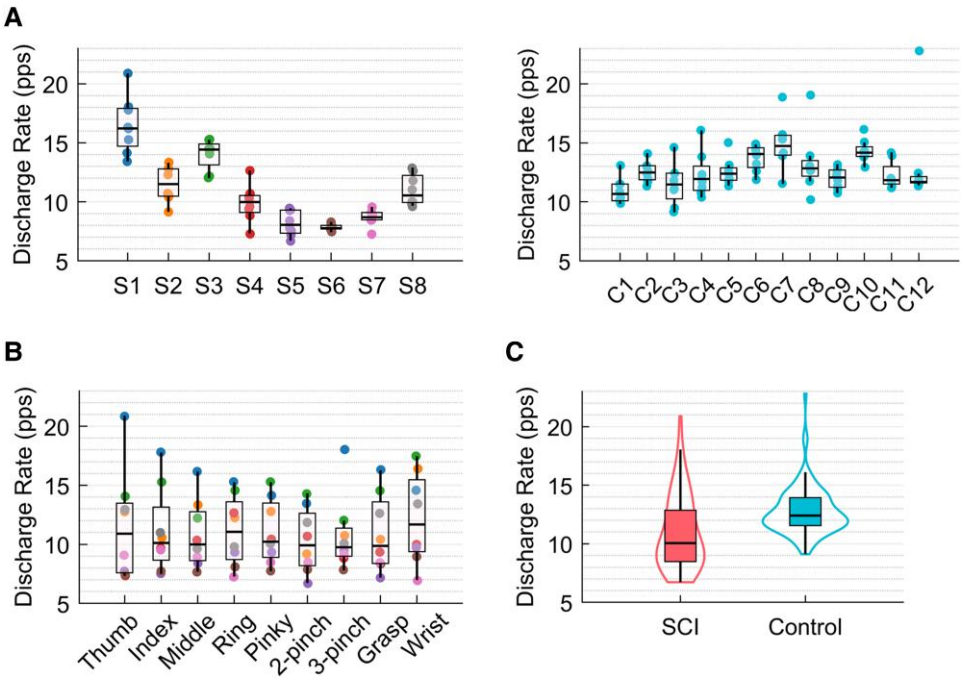

Figure 3 Discharge rate. (**A**) Average discharge rate across subjects for both groups [the dots are colour-coded for the subjects of the spinal cord injury (SCI) group]. (**B**) Average discharge rate across all tasks (the dots represent the tasks). (**C**) Distribution of the total number of motor units across groups, SCI in pink and control in blue.

stretch reflexes and spasticity are also presented in Table 1. We provide a comparison between raw EMG signals of SCI and control groups in Figs 2A and 6. For all the tasks (Fig. 2C and Table 1), we identified a specific subpopulation of motor units that encoded that particular movement, with an average of 9.8 ± 6.0 motor units per task across all SCI subjects. We also identified unique motor units for each task (Table 1). In Fig. 2B, we show the number of motor units across all tasks for each subject for SCI and control groups. Across tasks of the same subject, the variability in the number of motor units was low, with a standard deviation (SD) of between 1–2 motor units for all subjects except Subject S6 (SD = 4). For the control group, we observed an average of 8.0 ± 4.1 motor units per task across all participants. The groups present similar median values (Fig. 2D), with no significant difference regarding the number of decomposed motor units [generalized linear mixed-effects: $\beta = 0.007$, $t(144) = 1.10$, P-value = 0.27]. This information showed that the SCI subjects still presented a relatively high number of motor units.

Due to the similar number of identified motor units between the groups, we conducted an additional analysis to determine whether the HDsEMG data detected most of the active motor units in the SCI group. It is important to note that the number of detected motor units is not directly related to the total number of motor units, as many methodological factors influence it (see Del Vecchio *et al.*[20] and Oliveira *et al.*[21] for more information). First, we extracted the motor unit action potential shapes from the decomposed HDsEMG signals and convolved these shapes with the motor unit firings to reconstruct the EMG signal. We then calculated the root mean square error (RMSE) between the original and reconstructed EMG signals to measure the residual EMG activity (see the Supplementary Material, 'Methods' section). This value serves as an index of the undecomposed motor units and the total number of active motor units for a given task. Interestingly, as shown in Fig. 2E and F, we found significantly lower RMSE values in SCI (20.3 ± 16.7 μV) in comparison to the control (41.0 ± 18.8 μV) [$\beta = -33.7$, $t(144) = -4.5$, P-value = 1.6×10^{-5}]. These lower values indicate that we are decomposing a higher proportion of motor units in SCI and that there are fewer active motor units for a specific task.

In Fig. 3A and B, we present the average discharge rate in pulses per second (pps) calculated across tasks and subjects. We observed that the variation in discharge rate is subject-specific (Fig. 3A), with Subjects S1–S3 presenting higher median discharge rates. Comparing the data across subjects of both groups (average discharge rate of SCI = 11 ± 3.2 pps and control = 12.8 ± 2.1 pps per task across all subjects), we identified Subjects S4–S7 with the lower discharge rates, and Subjects S2, S3 and S8 with similar values to the control group. Overall, we observed no significant difference between the groups [$\beta = -0.002$, $t(144) = -1.64$, P-value = 0.10] (Fig. 3C).

In Fig. 4, we show the average coherence across all subjects and tasks and the area of each frequency bandwidth across subjects. For the delta band, the median area values did not differ across subjects apart from Subjects S1 and S6 (delta) with higher values. We found that Subjects S1 and S6 were significantly different from Subjects S3, S4 and S7 (Kruskal–Wallis's test: $H = 40.8$, df = 7, P-value = 8.7×10^{-7}). For the alpha band, only Subject S1 presented a higher median, being significantly different from Subjects S2, S4, S6 and S7 ($H = 25.2$, df = 7, P-value = 0.0007). For beta and gamma bands, Subjects S1, S3 and S5 presented higher coherence areas in comparison to the other subjects, the distributions from these subjects are significantly higher than Subject S2 (beta band, $H = 27.9$, df = 7, P-value = 0.0002). For gamma, we found Subject S3 to have the highest median, significantly different from Subjects S2, S4, S6 and S7; also, Subject S1 was significantly different from Subject S4 ($H = 35.4$, df = 7, P-value = 9.5×10^{-6}). When comparing between groups, only the beta and gamma bands were significantly higher in the SCI group—and this was only when we considered the tasks as a fixed effect in our generalized linear mixed-effects model

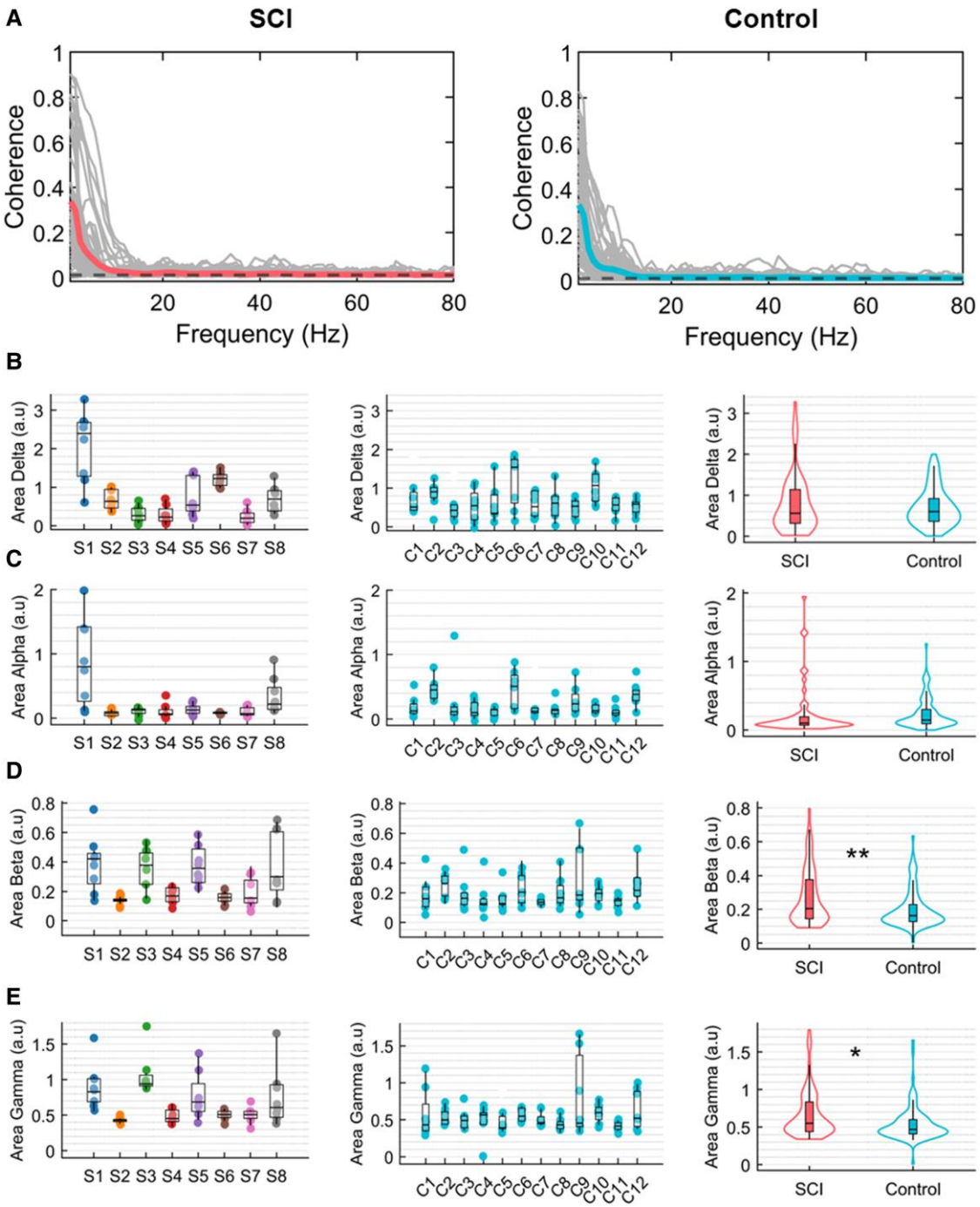

Figure 4 Coherence. (**A**) Average coherence across all participants and all tasks for both groups, spinal cord injury (SCI) in pink and control in blue. The black dashed line represents the coherence threshold (average coherence between 100–250 Hz). Each curve in grey represents the coherence for one subject. (**B–E**) Area under coherence curve across all subjects and groups for delta (1–5 Hz), alpha (6–12 Hz), beta (15–30 Hz) and gamma (31–80 Hz) bands, respectively (the dots represent the tasks and are colour-coded for the subjects of the SCI group). For each frequency band, we also show the group distribution of the coherence area values across all tasks and subjects. *$0.01 < P < 0.05$, **$0.001 < P < 0.01$.

(beta band: $\beta = 2.14$, $t(151) = 2.38$, P-value = 0.018; gamma band: $\beta = 0.73$, $t(151) = 2.75$, P-value = 0.007).

Overall, because of the number of motor units detected, we could identify unique units virtually in all recorded tasks (>2 motor units/task, except for Subject S3—Table 1), which allowed an accurate and precise classification for all these motor dimensions. Therefore, after years of cervical SCI leading to motor complete paralysis (ranging from 5.0 to 24.2 years; Table 1), these subjects still had spared connections from the motor cortex, impinging the activity of spinal motor neurons. This was evidenced by the fact that some motor units showed high voluntary modulation that matched with the kinematics of the virtual hand videos (Fig. 5A). Figure 5A shows all the identified motor units for all tasks of one individual. These previous results were based on the number of motor dimensions from the offline decomposition of the HDsEMG.

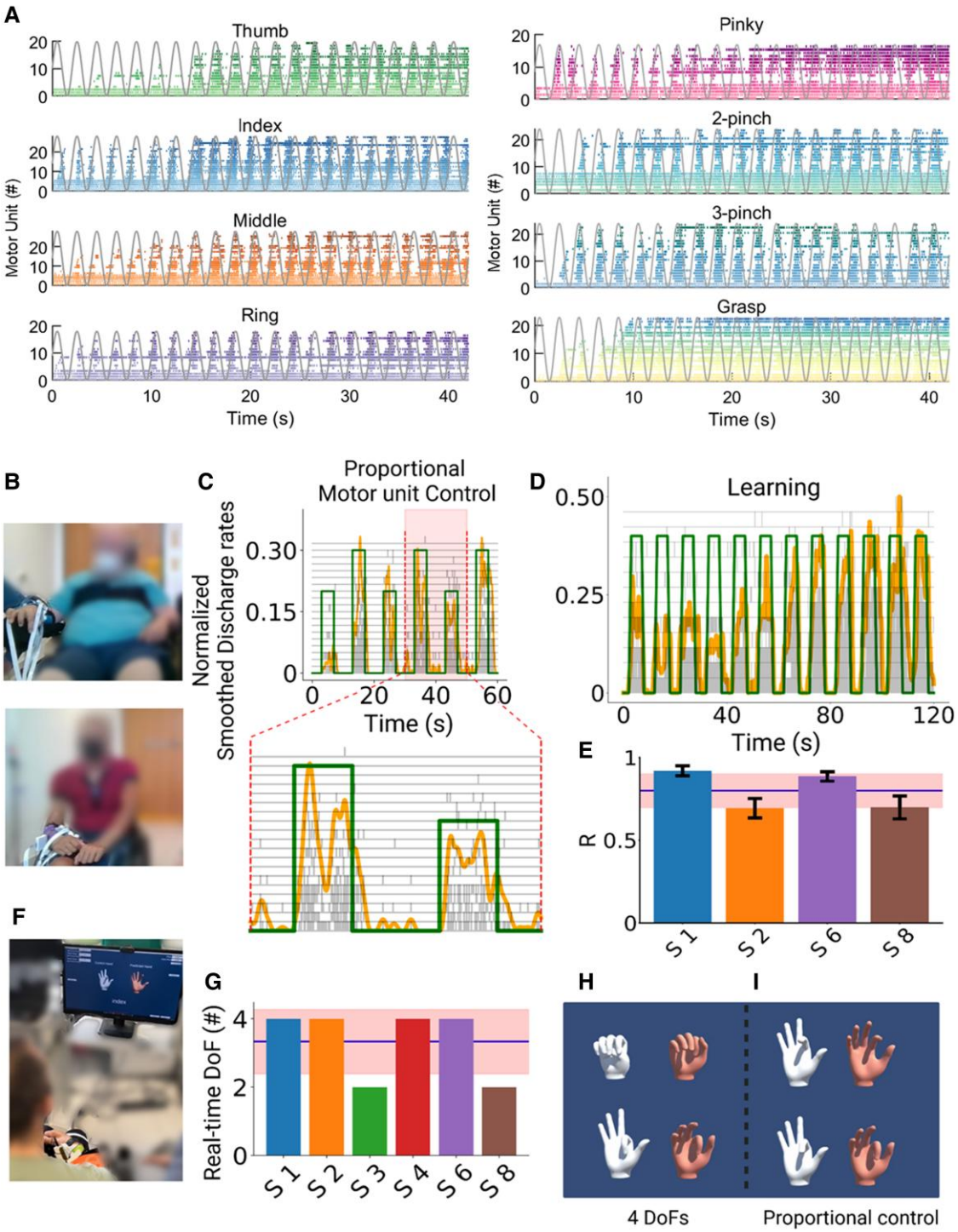

Figure 5 Real-time control of motor units and virtual hand. (**A**) Raster plot for all motor units identified for Subject S6 (S6) during the respective task (colour-coded) and the virtual hand movement trajectories (grey line). Note the task-modulated activity of the motor unit firing patterns that encoded flexion and extension movements. (**B**) Real-time tasks for two participants (Subjects S1 and S6). (**C**) The participants were asked to follow a trajectory on a screen (green line) by attempting a grasp movement. The motor units were decomposed online and the cumulative smoothed discharge rate (yellow line) was used as biofeedback. After a few seconds of training (**D**), the subjects could track the trajectories with high accuracy and at different target levels (**C**). (**E**) Cross-correlation coefficient (R) between the smoothed discharge rate and the requested tasks for four subjects. (**F**) After the online motor unit decomposition, we used a supervised machine learning method to proportionally control the movement of a virtual hand. Four of six subjects were able to proportionally open and close the hand (**G–I**) and proportionally control in both movement directions (flexion and extension) the index finger (**H** and **I**). These subjects were able to control four degrees of freedom (DoFs) that corresponded to hand opening, closing, index flexion and extension. These subjects were able to control four DoFs that corresponded to hand opening, closing, index flexion and extension.

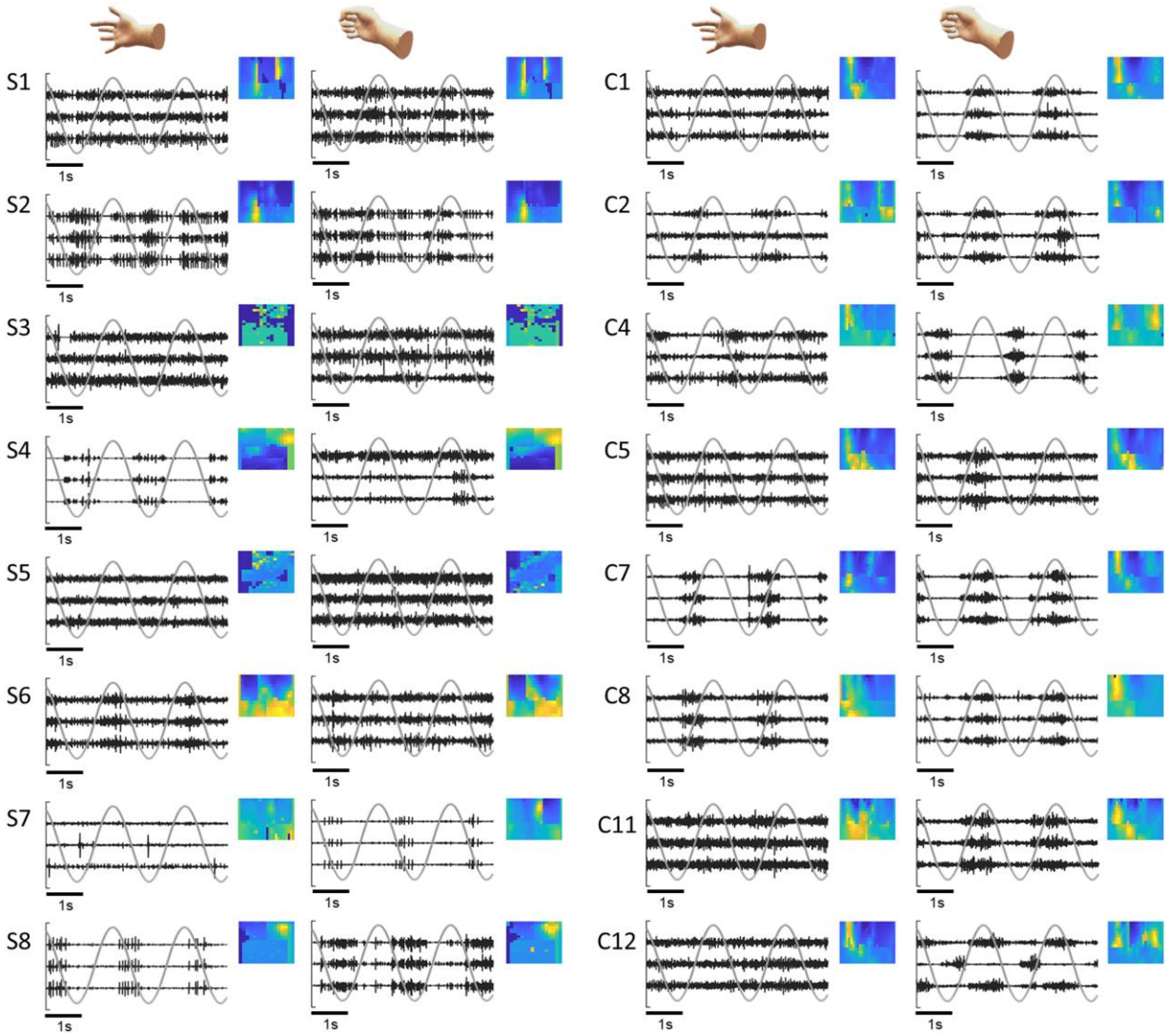

Figure 6 Examples of raw high-density surface electromyograph (HDsEMG) signals and spatial amplitude maps. We report examples of EMG signals for all subjects of the spinal cord injury (SCI) group (S1–S8) during index and grasp tasks. The normalized signals from the three EMG channels with higher root mean square (RMS) values (in black) are presented over 5 s, together with the virtual hand kinematics (in grey). For each subject, we show a spatial map based on the RMS values of each EMG channel. For brevity, we only present data from eight control group participants for comparison.

In a second experiment, on average 3–5 months after the first session, we tested six subjects again (Subjects S1–S4, S6 and S8) with a similar experimental procedure but tuned for real-time control. We asked the subjects to proportionally control a moving cursor on a screen based on the real-time decoding of the discharge timings of motor neurons (Fig. 5C and D). Moreover, these individuals also controlled a virtual hand (Fig. 5F–I and Supplementary Video 2), demonstrating full voluntary control of the decoded neural activity.

We developed a real-time mapping of the discharge timings of motor neurons so that the patients could control a cursor on the screen with the motor unit discharge activity and a virtual hand with the HDsEMG signals (Fig. 5 and Supplementary Video 1). After a few seconds of training (Fig. 5D), the subjects were able to control the motor unit firing patterns and progressive recruitment of motor units at different target forces and with high accuracies, i.e. high cross-correlation values between the requested trajectory and the smoothed cumulative motor unit discharge rate (Fig. 5C and D). In this experiment, we also used a supervised machine learning algorithm to control a virtual hand (Fig. 5F–I and Supplementary Video 2).

Supplementary Video 1 shows a subject controlling the activity of groups of motor units in real time, modulating the recruitment and discharge rate to proportionally match two different target levels of activation. The motor neuron discharge times were summed and normalized in real time to the number of active neurons so that the patients could modulate a moving object (yellow cursor; Fig. 5C and D) by increasing/decreasing the discharge rates. Figure 5C shows the proportional control of two target levels mediated by both the concurrent recruitment of additional units (grey raster plot) and higher discharge rates. Figure 5D shows a complete recording set that lasted 120 s. Note that just after 50 s of training, the subject was able to move the cursor on relatively high levels of normalized motor unit activity. The scaling of the motor unit activity is based on an equation that considers the maximal motor unit discharge activity and the highest number of motor units identified during an offline calibration trial that lasted 10 s for each trained task.

We then trained the subjects to move a virtual hand that was displayed on a monitor and to match the movement of a control hand (Fig. 5F–I and Supplementary Video 2). After this training, the subjects could proportionally and repeatedly open and close the hand, when compared to the control hand instructions (Fig. 5I and Supplementary Video 2). Most of the participants were able to proportionally flex and extend the index finger (2 df) and open and close the hand (2 df). Figure 5F shows the subject's view: the monitor displayed two hands, a control hand (white colour) and a second hand controlled by a regression-based machine learning algorithm. Four of six subjects (Fig. 5G) were able to control f4 df, consisting of proportional control of index flexion and extension and hand opening and closing (Fig. 5H and I and Supplementary Video 2).

Discussion

The results above confirm previous evidence of voluntarily controlled spinal motor neurons in subjects with SCI (motor complete ranging from C5 to C6) that have been paralysed for decades.[7-10] We observed the presence of active modulation of motor neuron activity in all tested patients, with motor units associated with flexion or extension of movements of the paralysed hand digits. This association was evidenced by the real-time proportional control of the spinal motor neurons, complex movements of the virtual hand and the factorization analysis results, in which two modules (flexion and extension) explained most of the variance for the movements of each subject. Although the power spectrum of the extracted neural modules shows a peak at the movement frequency, these modules seem to be relatively out of phase and/or delayed for some tasks. These offline results agreed with our previous single-case study.[8]

Although there was variability in the number of identified motor units across subjects, this number was statistically comparable to the number of motor units found in the control group. For several reasons, we hypothesized that more motor units would be detected for the SCI group. First, the decomposition of HDsEMG signals relies on the total number of active motor units, so the higher this number, the more complex it is for the algorithm to separate the individual motor units[20,21] (for example, in healthy individuals, we detect more motor units at 10% of maximal force than at 50%, due to a higher superimposition of higher, larger-threshold motor units). Second, the algorithm works best when there are minimal muscle movements (due to the gearing of the muscle) below the recording electrodes. In the SCI group, due to paralysis, this condition was guaranteed as there was no visible movement or force during the attempted hand movements. Moreover, because of the spinal lesion, the number of motor units that the SCI individuals could voluntarily recruit was low, leading to low background noise on the EMG. In contrast, the control group was likely to have a higher number of motor units recruited. Consequently, from a computational perspective, this would allow better detection of motor units by decomposition algorithms. Although we found a high number of motor units for two subjects (Subjects S1 and S6; Table 1) with different characteristics (e.g. age, injury), this was not observed for the rest of the SCI group. This might indicate a lower number of active motor units for the other subjects of this group.

We further conducted an analysis comparing the filtered-original EMG and the reconstructed EMG. By reconstructing the EMG using the decomposed motor units, we could estimate the residual EMG activity, which is related to the motor units that are not decomposed. As anticipated, we found that the SCI subjects showed smaller RMSE values than the control group, suggesting that we likely decomposed the majority of the spared motor units present in the EMG signal.

The discharge rate was highly variable across subjects and tasks, with three participants presenting a higher median discharge rate than the others. The discharge rate across tasks varied from 7–21 pps, and it was comparable with our control group. Even though the absence of visible movement, the motor unit discharges were still within the range for voluntary contractions in non-injured healthy young adults.[22] This finding supported the idea that the discharge rate can be applied as user feedback for controlling the proposed interface.

The coherence values indicated that the motor neurons shared common synaptic inputs, and therefore, a few active motor neurons can be representative of a large pool of motor neurons and used for decoding. In the SCI group, we did not observe a clear pattern of coherence area across subjects. Some subjects presented concurrently higher beta and gamma coherence than others, influencing the comparison across groups, with beta and gamma being higher than in the control group. Previous literature describes a possible decrease in beta, with reduced corticospinal input after SCI, and an increase in gamma coherence as compensatory.[23-26] However, a few potential limitations should be considered. First, our results should be validated by a larger number of participants. Second, the coherence values included both intramuscular and intermuscular coherence. Therefore, we were not able to distinguish the motor units from specific motor pools. Last, we could not perform motor-evoked potential measurements, and further electrophysiological measurements are necessary to assess the function and integrity of corticospinal pathways.

Despite that, beta coherence was significantly associated with cortical control since peripheral beta coherence has been shown to be correlated with EEG cortical beta during voluntary movements.[27] In addition, beta activity has also been shown to be volitionally modulated through neurofeedback, which could be applied in training SCI participants.[27] Future experiments, including motor-evoked potentials[28,29] and other experimental paradigms[30,31] could highlight potential differences in descending pathways from the cortex and brainstem in controlling flexors and extensor motor units.

Additionally, we did not observe any specific relationships between the behaviour of the active motor units (discharge rate, coherence) and the spasticity level, stretch reflex and sensory level of the injury obtained from clinical examinations. However, this may be attributed to the variability between subjects and the relatively low number of tested patients ($n = 8$). Since we have no more information on the residual sensory and motor pathways, we are limited to understanding which characteristics could be related to this residual voluntary control. This should be examined in future studies.

Regarding the number of motor units for each task, overall, we found at least two unique motor units per task, except for Subject S3 (Fig. 2 and Table 1). The unique motor units were defined as motor units that are recruited only during one attempted movement. Once they are activated, we can be sure that the SCI individual is attempting a specific movement. This finding confirmed that the motion intent of individuals with SCI can be decoded through our non-invasive interface. According to our real-time tests and previous work,[8] at least one to two unique motor units per task are necessary for our detection approach and to be able to decode more complex movements. The number of detected motor units for each task is crucial for the neural interface performance. The number

of unique motor units influences the classification of specific motor dimensions (e.g. index versus middle finger tasks) and the stability of the control over time. It is important to note that a decreased error in the control is observed with more decoded units due to the averaging effects caused by a large number of motor units firing synchronously.[32]

Finally, given the number of specific task-modulated motor units found, we developed a real-time mapping of the discharge timings of motoneurons so that the patients could control a cursor on a monitor and a virtual hand, through an EMG-to-activation regression model. The tested patients performed both cursor and virtual hand tasks accurately and proportionally, demonstrating full voluntary control of the decoded neural activity with the ability to modulate the motor units' discharge rate. Interestingly, all the patients could proportionally control the cursor to 20% and 30% of maximal activation. For the control of a prosthetic device, the proportional control of a motor unit firing activity from 1% to 30% would be sufficient to obtain a large output of forces that could be controlled with, for example, a brushless motor. Therefore, this relatively low range should not indicate a problem in the method but rather a strength of the approach.

Regarding the virtual hand control, this approach is based on a linear regressor model, including an adaptive filter,[33] that learns and maps combinations of EMG activity into the movement of the virtual hand. To build the regressor model, we defined artificial labels associated with the movements. Therefore, independent of the capabilities of the user, there is a possible linear superposition of the output labels used during the training of the machine learning model due to the similarity between EMG patterns related to the different movements. Consequently, some accessory movements of the virtual hand might occur. For this reason, the virtual hand control performance was evaluated simply by task completion.[34,35]

Moreover, it is important to note that no extensive training was required from the subjects when performing the tasks. Each experiment across all patients did not last more than 3 h, and we used most of this time to place the electrodes and explain the tasks. Although we did not measure the time it took for the subjects to control the virtual hand and 2D cursor control, we estimate less than 30 min, even for the individuals with the highest level of wrist and hand paralysis. This time can be further improved once the subjects are trained with the tasks. A critical aspect of neural interfaces is the training time and intuitive use. The fact that the subjects learned the tasks in a short training time and were not under fatigue conditions demonstrates the feasibility of the presented approach.

Our results indicated that motor- and sensory-complete SCI individuals maintain relevant neural activity as the output of the spinal cord circuits below the lesion and that they can accurately control this activity to regain hand function. Wearable muscle sensors are accessible, non-invasive and have the potential to enhance the neural control of assistive devices and increase the use of these devices. Therefore, this technology may compete in terms of clinical viability and efficacy with current invasive brain or spine implants for restoring hand function in complete SCI patients. While we cannot directly compare these approaches and further tests are needed, our results are similar in task achievement and performance for tasks such as grasping and other hand movements without requiring any surgery and complex models.[36-38] Previous surveys have shown that a considerable number of tetraplegic and paraplegic patients are reluctant to have cortical implants.[3,39,40] Therefore, we argue that the proposed non-invasive approach might have the potential to be a clinically superior solution for the purpose of hand function restoration in SCI compared with current invasive brain and spinal neural interfaces.

One important constraint of our approach is that it is inherently linked to spared motor unit activity. Although we found spared motor units in all SCI individuals that were classified as motor complete, this technology may not be effective for subjects with higher levels of complete lesions (C1–C2) and muscles far from the level of the injury. A second constraint is that we calibrate our real-time sessions in an offline decomposition step by decoding the activity during a predefined task. This implies that the online decomposition is limited by the number of motor units recruited during this first step. Therefore, it is possible that motor units recruited during real-time tasks cannot be detected by our algorithms. This could be further improved by implementing algorithms that work in parallel with the real-time feedback of motor unit data to the patients. Importantly, for the classification of the different hand digit movements, our method is inherently bound to the number of unique motor units that can be found in a task. Furthermore, spasticity could also affect the efficiency of our approach. We observed that some motor units persist in firing even when the voluntary intent stops, and this should also be considered for the development of future algorithms.

Limitations

This study focused on HDsEMG measurements, motor unit behaviour and real-time control of motor unit activity. Therefore, this limited the investigation of the mechanisms underlying the residual voluntary activity found in SCI subjects. As spinal motor neurons execute the final motor commands, we have limited information on the spinal and supraspinal inputs that determine the volitional recruitment and modulation of motor unit firings in SCI. Additional electrophysiological and clinical tests, such as stimulation of the brain and spinal cord, might help to infer some of the cortical and spinal pathways involved. Consequently, with the current dataset, we cannot hypothesize about the origins of the synaptic inputs impinging on spinal motor neurons. Future tests should include further medical examinations concurrent with electrophysiological testing at the central and peripheral levels and evoked electrical and magnetic stimulation measurements.

Conclusion

In summary, our results confirmed that SCI subjects can voluntarily control residual motor neuron activity. This activity provides enough information to decode the movement intent of fine hand tasks. We demonstrated that the presented non-invasive technology could provide intuitive and effective control of the paralysed hand, even many years after the injury. Our findings could be helpful in the investigation of movement control and recovery mechanisms after SCI through the tracking of the same motor unit across interventions. Therefore, this neural interface has a direct clinical translation for home and hospital use to restore and monitor the spared connections after traumatic SCI. Further work will focus on improving the online control based on motor unit activity related to the different movements and integration with assistive technologies such as exoskeletons and prosthetics.

Data availability

The data that support the findings of this study are available from the corresponding author, upon reasonable request.

Acknowledgements

We would like to thank all participants of this study, especially the ones from the SCI group whose efforts made this study possible.

Funding

This work was supported by the European Research Council (ERC) Starting Grant project GRASPAGAIN under grant 101118089 (A.D.V.); the German Ministry for Education and Research (BMBF) through the project MYOREHAB under Grant 01DN2300 (A.D.V.); Bavarian State Ministry of Economic Affairs and Media, Energy and Technology through the project NeurOne under grant LSM-2303-0003 (A.D.V.) and the d.hip (Digital Health Innovation Platform), a cooperation between Siemens Healthineers, Medical Valley, University Hospital Erlangen (Universitätsklinikum Erlangen) and Friedrich-Alexander University (Friedrich-Alexander-Universität Erlangen-Nürnberg) (A.D.V.). D.F. is funded by the European Research Council (ERC) under the Synergy Grant Natural BionicS (810346) and Engineering and Physical Sciences Research Council EPSRC Transformative Healthcare for 2050 project NISNEM Technology (EP/T020970/1).

Competing interests

The authors report no competing interests.

Supplementary material

Supplementary material is available at *Brain* online.

References

1. Snoek GJ, Ijzerman MJ, Hermens HJ, Maxwell D, Biering-Sorensen F. Survey of the needs of patients with spinal cord injury: Impact and priority for improvement in hand function in tetraplegics. *Spinal Cord*. 2004;42:526-532.
2. Fridén J, House J, Keith M, Schibli S, van Zyl N. Improving hand function after spinal cord injury. *J Hand Surg Eur*. 2022;47:105-116.
3. Collinger JL, Boninger ML, Bruns TM, Curley K, Wang W, Weber DJ. Functional priorities, assistive technology and brain-computer interfaces after spinal cord injury. *J Rehabil Res Dev*. 2013;50:145-160.
4. Bouton CE, Shaikhouni A, Annetta NV, et al. Restoring cortical control of functional movement in a human with quadriplegia. *Nature*. 2016;533:247-250.
5. Benabid AL, Costecalde T, Eliseyev A, et al. An exoskeleton controlled by an epidural wireless brain–machine interface in a tetraplegic patient: A proof-of-concept demonstration. *Lancet Neurol*. 2019;18:1112-1122.
6. Barra B, Conti S, Perich MG, et al. Epidural electrical stimulation of the cervical dorsal roots restores voluntary upper limb control in paralysed monkeys. *Nat Neurosci*. 2022;25:924-934.
7. Sherwood AM, Dimitrijevic MR, McKay WB. Evidence of subclinical brain influence in clinically complete spinal cord injury: Discomplete SCI. *J Neurol Sci*. 1992;110(1–2):90-98.
8. Ting JE, Del Vecchio A, Sarma D, et al. Sensing and decoding the neural drive to paralysed muscles during attempted movements of a person with tetraplegia using a sleeve array. *J Neurophysiol*. 2021;127:2104-2118.
9. Sharma P, Naglah A, Aslan S, et al. Preservation of functional descending input to paralysed upper extremity muscles in motor complete cervical spinal cord injury. *Clin Neurophysiol*. 2023;150:56-68.
10. Wahlgren C, Levi R, Amezcua S, Thorell O, Thordstein M. Prevalence of discomplete sensorimotor spinal cord injury as evidenced by neurophysiological methods: A cross-sectional study. *J Rehabil Med*. 2021;53:jrm00156.
11. Del Vecchio A, Sylos-Labini F, Mondì V, et al. Spinal motoneurons of the human newborn are highly synchronized during leg movements. *Sci Adv*. 2020;6:eabc3916.
12. Del Vecchio A, Germer CM, Elias L, et al. The human central nervous system transmits common synaptic inputs to distinct motor neuron pools during non-synergistic digit actions. *J Physiol*. 2019;597:5935-5948.
13. Farina D, Holobar A. Characterization of human motor units from surface EMG decomposition. *Proc IEEE*. 2016;104:353-373.
14. Mendez Guerra I, Barsakcioglu DY, Vujaklija I, Wetmore DZ, Farina D. Far-field electric potentials provide access to the output from the spinal cord from wrist-mounted sensors. *J Neural Eng*. 2022;19:026031.
15. Cakici AL, Osswald M, De Oliveira DS, et al. A generalized framework for the study of spinal motor neurons controlling the human hand during dynamic movements. *Annu Int Conf IEEE Eng Med Biol Soc EMBS*. 2022;2022:4115-4118.
16. Fuglevand AJ, Lester RA, Johns RK. Distinguishing intrinsic from extrinsic factors underlying firing rate saturation in human motor units. *J Neurophysiol*. 2015;113:1310-1322.
17. Enoka RM. Physiological validation of the decomposition of surface EMG signals. *J Electromyogr Kinesiol*. 2019;46:70-83.
18. Heckman CJ, Enoka RM. Motor unit. *Compr Physiol*. 2012;2:2629-2682.
19. Holobar A, Minetto MA, Farina D. Accurate identification of motor unit discharge patterns from high-density surface EMG and validation with a novel signal-based performance metric. *J Neural Eng*. 2014;11:016008.
20. Del Vecchio A, Holobar A, Falla D, Felici F, Enoka RM, Farina D. Tutorial: Analysis of motor unit discharge characteristics from high-density surface EMG signals. *J Electromyogr Kinesiol*. 2020;53:102426.
21. Oliveira DS, Casolo A, Balshaw TG, et al. Neural decoding from surface high-density EMG signals: Influence of anatomy and synchronization on the number of identified motor units. *J Neural Eng*. 2022;19:046029.
22. Moritz CT, Barry BK, Pascoe MA, Enoka RM. Discharge rate variability influences the variation in force fluctuations across the working range of a hand muscle. *J Neurophysiol*. 2005;93:2449-2459.
23. Proudfoot M, van Ede F, Quinn A, et al. Impaired corticomuscular and interhemispheric cortical beta oscillation coupling in amyotrophic lateral sclerosis. *Clin Neurophysiol*. 2018;129:1479-1489.
24. Fisher KM, Zaaimi B, Williams TL, Baker SN, Baker MR. Beta-band intermuscular coherence: A novel biomarker of upper motor neuron dysfunction in motor neuron disease. *Brain*. 2012;135:2849-2864.
25. Norton JA, Gorassini MA. Changes in cortically related intermuscular coherence accompanying improvements in locomotor skills in incomplete spinal cord injury. *J Neurophysiol*. 2006;95:2580-2589.
26. Nishimura Y, Morichika Y, Isa T. A subcortical oscillatory network contributes to recovery of hand dexterity after spinal cord injury. *Brain*. 2009;132:709-721.

27. Bräcklein M, Barsakcioglu DY, Del Vecchio A, Ibáñez J, Farina D. Reading and modulating cortical β bursts from motor unit spiking activity. *J Neurosci*. 2022;42:3611-3621.
28. Raptis H, Burtet L, Forget R, Feldman AG. Control of wrist position and muscle relaxation by shifting spatial frames of reference for motoneuronal recruitment: Possible involvement of corticospinal pathways. *J Physiol*. 2010;588:1551-1570.
29. Long J, Federico P, Perez MA. A novel cortical target to enhance hand motor output in humans with spinal cord injury. *Brain*. 2017;140:1619-1632.
30. Baker SN, Perez MA. Reticulospinal contributions to gross hand function after human spinal cord injury. *J Neurosci*. 2017;37:9778-9784.
31. Baker SN. The primate reticulospinal tract, hand function and functional recovery. *J Physiol*. 2011;589:5603-5612.
32. Barsakcioglu DY, Bracklein M, Holobar A, Farina D. Control of spinal motoneurons by feedback from a non-invasive real-time interface. *IEEE Trans Biomed Eng*. 2021;68:926-935.
33. Sierotowicz M, Scheidl MA, Castellini C. Adaptive filter for biosignal-driven force controls preserves predictive powers of sEMG. *IEEE Int Conf Rehabil Robot*. 2023;2023:1-6.
34. Simon AM, Hargrove LJ, Lock BA, Kuiken TA. Target Achievement Control Test: Evaluating real-time myoelectric pattern-recognition control of multifunctional upper-limb prostheses. *J Rehabil Res Dev*. 2011;48:619.
35. Nowak M, Vujaklija I, Sturma A, Castellini C, Farina D. Simultaneous and proportional real-time myocontrol of up to three degrees of freedom of the wrist and hand. *IEEE Trans Biomed Eng*. 2023;70:459-469.
36. Bockbrader M, Annetta N, Friedenberg D, et al. Clinically significant gains in skillful grasp coordination by an individual with tetraplegia using an implanted brain-computer interface with forearm transcutaneous muscle stimulation. *Arch Phys Med Rehabil*. 2019;100:1201-1217.
37. Simeral JD, Kim SP, Black MJ, Donoghue JP, Hochberg LR. Neural control of cursor trajectory and click by a human with tetraplegia 1000 days after implant of an intracortical microelectrode array. *J Neural Eng*. 2011;8:025027 .
38. Wandelt SK, Kellis S, Bjånes DA, et al. Decoding grasp and speech signals from the cortical grasp circuit in a tetraplegic human. *Neuron*. 2022;110:1777-1787.e3.
39. Blabe CH, Gilja V, Chestek CA, Shenoy KV, Anderson KD, Henderson JM. Assessment of brain-machine interfaces from the perspective of people with paralysis. *J Neural Eng*. 2015;12:043002.
40. Lahr J, Schwartz C, Heimbach B, Aertsen A, Rickert J, Ball T. Invasive brain-machine interfaces: A survey of paralysed 'patients' attitudes, knowledge and methods of information retrieval. *J Neural Eng*. 2015;12:043001.